



LAWRENCE
LIVERMORE
NATIONAL
LABORATORY

LLNL-TR-637972

Reaction Between Thin Gold Wires And Pb-Sn-In
Solder (37.5%, 37.5%, 25%), Part C. A
Comprehensive Model Of The Reaction Inside
The Solder Mounds In Both The Interface
Controlled Regime And The Diffusion-Controlled
Regime.

W. J. Siekhaus

May 31, 2013

Disclaimer

This document was prepared as an account of work sponsored by an agency of the United States government. Neither the United States government nor Lawrence Livermore National Security, LLC, nor any of their employees makes any warranty, expressed or implied, or assumes any legal liability or responsibility for the accuracy, completeness, or usefulness of any information, apparatus, product, or process disclosed, or represents that its use would not infringe privately owned rights. Reference herein to any specific commercial product, process, or service by trade name, trademark, manufacturer, or otherwise does not necessarily constitute or imply its endorsement, recommendation, or favoring by the United States government or Lawrence Livermore National Security, LLC. The views and opinions of authors expressed herein do not necessarily state or reflect those of the United States government or Lawrence Livermore National Security, LLC, and shall not be used for advertising or product endorsement purposes.

This work performed under the auspices of the U.S. Department of Energy by Lawrence Livermore National Laboratory under Contract DE-AC52-07NA27344.

Reaction Between Thin Gold Wires And Pb-Sn-In Solder (37.5%, 37.5%, 25%),
Part C. A Comprehensive Model Of The Reaction Inside The Solder Mounds In Both
The "Interface Controlled Regime" And The "Diffusion-Controlled" Regime.

Wigbert J. Siekhaus

This work was performed under the auspices of the U.S.
Department of Energy by Lawrence Livermore National Laboratory
in part under Contract W-7405-Eng-48 and in part under Contract
DE-AC52-07NA27344.

C.I) Introduction

In part A, all available literature data are displayed in tables, and plotted in figure 1. The slopes of the lines through the data in figure 1 suggest that there is a change in the rate controlling mechanism from interface control (linear with time, slope equals one in figure 1) to diffusion control (proportional to square root of time, slope one half in figure 1) as the gold consumption increases. Here we develop a model for the diffusion-controlled reaction using data from planar and circular geometry. We determine the regimes in time and temperature where the reaction is diffusion controlled and where it is interface controlled, and then derive the set of equations for a comprehensive time and temperature dependent model that describes the reaction for all temperatures and time.

C.II) Using all available data to develop a diffusion-controlled reaction

model.

The change in mechanism from interface control to diffusion control suggested in figure 1 appears to be temperature dependent. If one extends the line through Yost et al.'s data at 150°C until it intersects the line through the 151°C data of Powell & Braun, one would estimate that this change in rate mechanism occurs at that temperature when the gold consumption is about 50 μm . Braun & Rhinehammer's data in figure 1 suggest that at lower temperatures this change in reaction rate control mechanism may occur at gold consumption below 10 μm . There are, however, only very few data available that clearly show diffusion control. That makes it difficult to develop a model that can be trusted. To demonstrate the change in the rate controlling mechanism we plot in figure 28 all data of Yost et al. [9], generated in planar geometry.

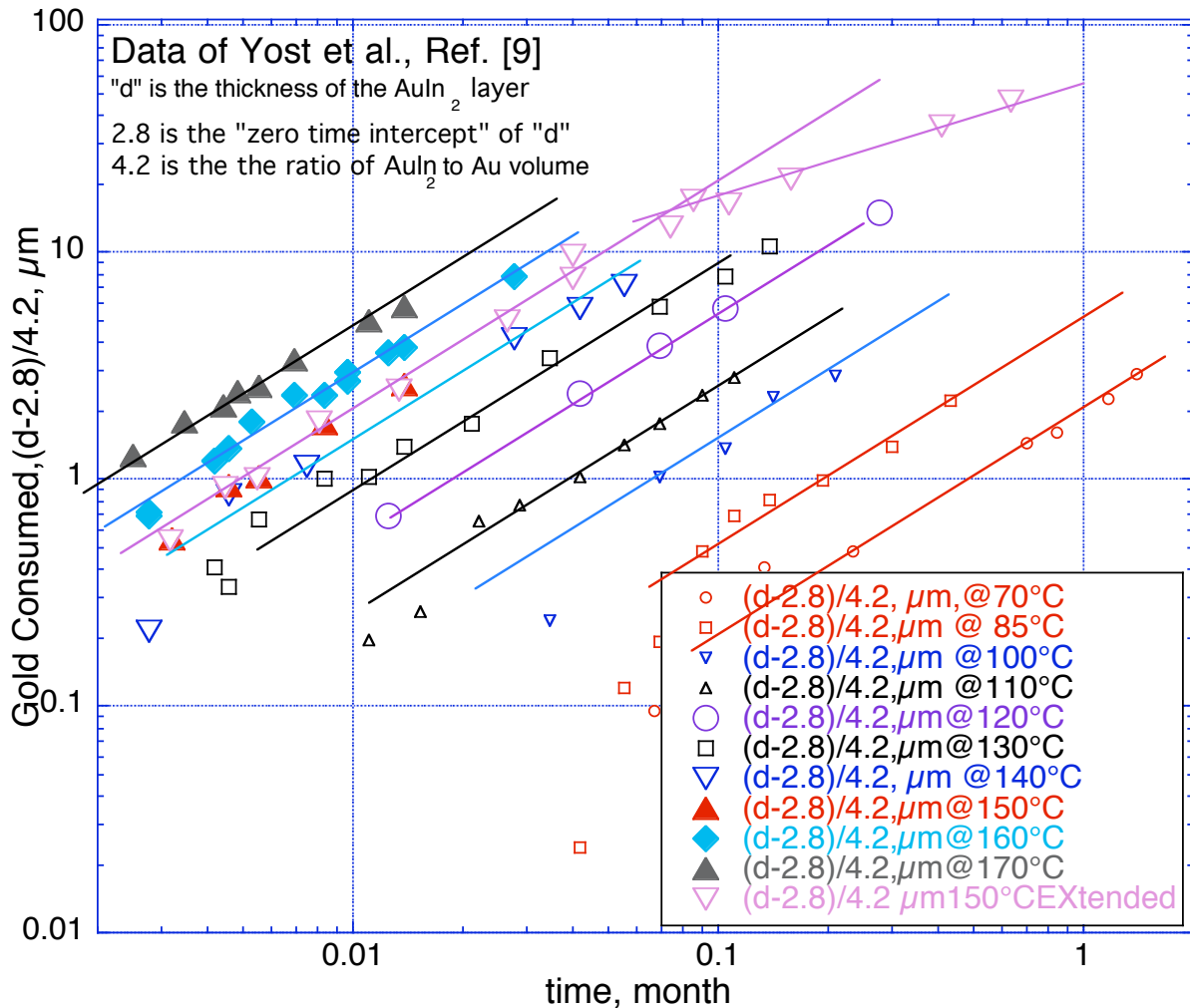


Figure 28. Gold consumption versus time in planar geometry, using data of Yost

et al. [9]. The gold consumption is calculated by converting the AuIn_2 thickness observed by Yost et al. to the equivalent of gold. Yost et al.'s "d" data have an "average" zero time intercept of $2.8\mu\text{m}$. That "average" intercept is subtracted from the data in this graph, which leads to the deviation from linear behavior for some of the y-axis data below $.2\mu\text{m}$. The data of most interest here are the two sets of data at 150°C . There are two points of interest: 1) the data are very reproducible: the filled red triangles and the empty purple triangles coincide, 2) the data above about $20\mu\text{m}$ show a distinctly different slope (i.e. $\frac{1}{2}$, implying that the reaction is proportional to $\sqrt{\text{time}}$, diffusion controlled, in that regime.) The data of most interest here are the two sets of data at 150°C . (The second set of data at 150°C , shown in figure 14 of Yost et al. are NOT shown in figure 1). There are two points of interest: 1) the data are very reproducible: the filled red triangles (set 1) and the empty purple triangles (set 2) coincide, 2) the data above $10\mu\text{m}$ show a distinctly different slope (i.e. $\frac{1}{2}$, implying that the reaction in that regime is proportional to square root of time, diffusion controlled.) The linear and non-linear slopes intersect at approximately $20\mu\text{m}$. There is another set of data in planar geometry by Powell and Braun [8]. In figure 29 the data of Powell and Braun are plotted vs. square root of time, together with the 150°C data of Yost et al. The equations fitted to the data are also shown. In order to develop a temperature dependent model for the diffusion controlled reaction the coefficients multiplying "square root of time" should be known over a wide range of temperatures. Unfortunately only one additional set of data for gold consumption above $20\mu\text{m}$ exists, measured at LLNL for gold wires of $101.6\mu\text{m}$ diameter at 79.9 and at 90.9°C , shown in figure 30 as a function of square root of time. Only one single data point exists at 79.9°C .

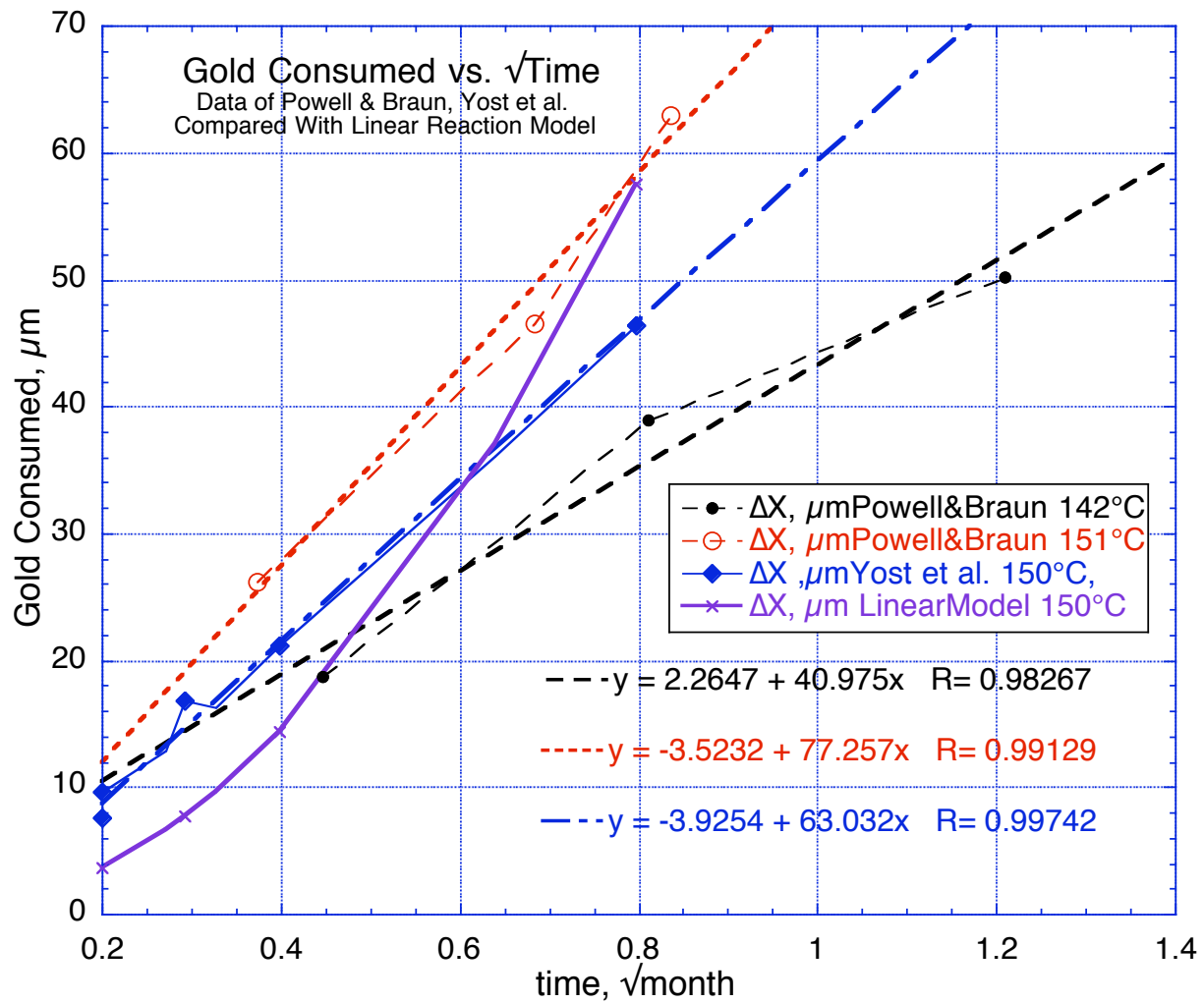


Figure 29. Gold consumption versus square root of time in planar geometry. Data at 150°C of Yost et al. [9] for gold consumption greater than about 10 μm plotted versus square root of exposure time, together with the data of Powell and Braun [8] at 142 and 151°C. Both data sets are well fitted with equations proportional to square root of time, indicating that in this regime the reaction is diffusion controlled. The rates of reaction per square root of month are 40.975 at 142°C and 77.257 at 151°C respectively for Powell and Braun's data, and 63.032 for Yost et al.' data. Also shown is the gold consumption predicted by the linear reaction model. It intersects the data at 142°C at about 22 μm , and the data at 150°C and 151°C at 34 and 55 μm respectively.

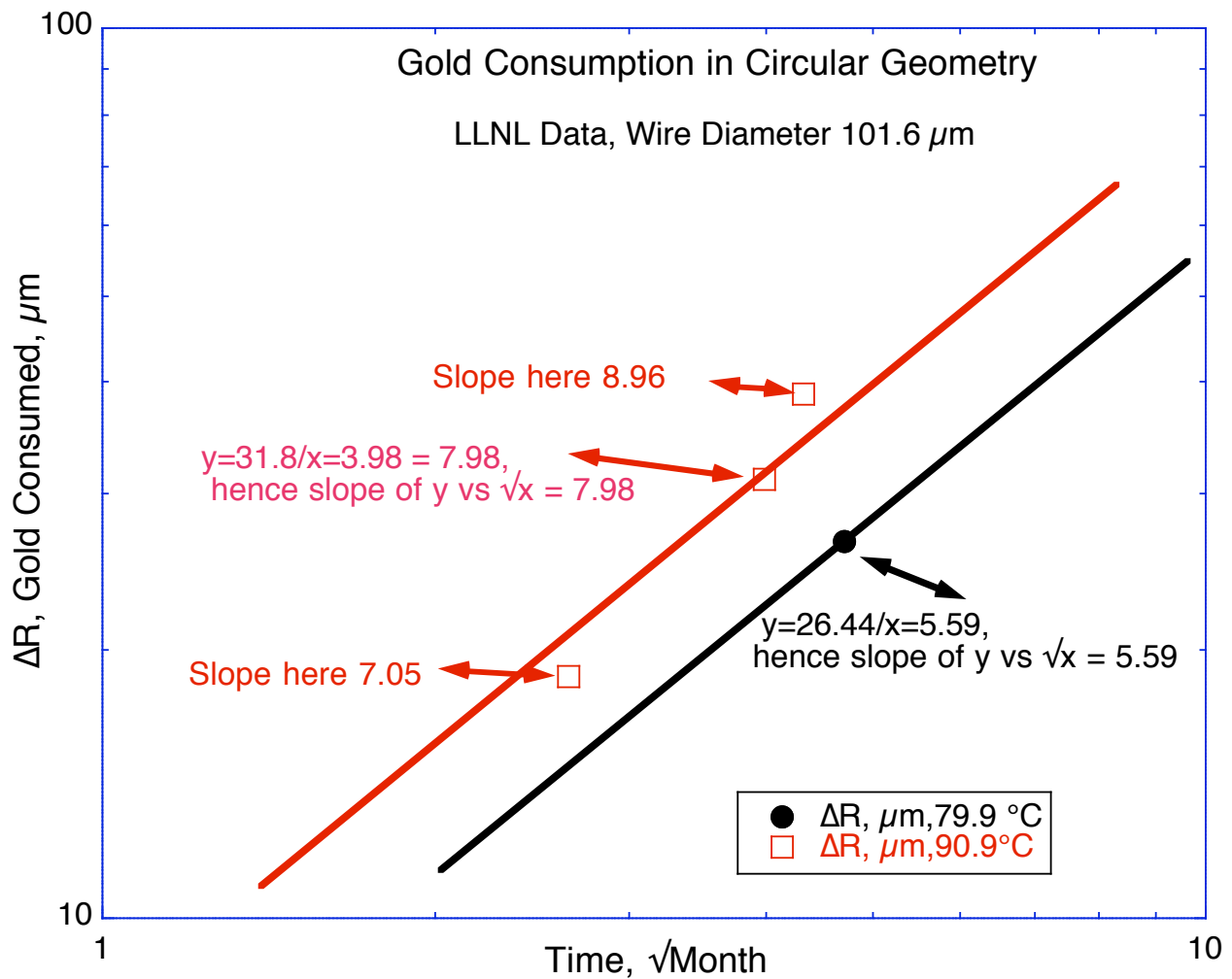


Figure 30. Gold consumption measured at Lawrence Livermore

National Laboratory on wires of 101.6 μm diameters plotted in a double logarithmic graph as a function of square root of time. Only one data point exist for 79.9 °C, and only three data points at 90.9 °C. Therefore no fit "linear with $\sqrt{\text{time}}$ " is done, but rather lines "linear with $\sqrt{\text{time}}$ " are drawn in this log-log plot to demonstrate that the measured values are consistent with diffusion control, and the "slopes" are calculated at each data point.

The coefficients multiplying square root of time are calculated or derived in figure 30 (see details there), and used in figure 31 in an Arrhenius plot to derive the model equation describing the diffusion-controlled reaction.

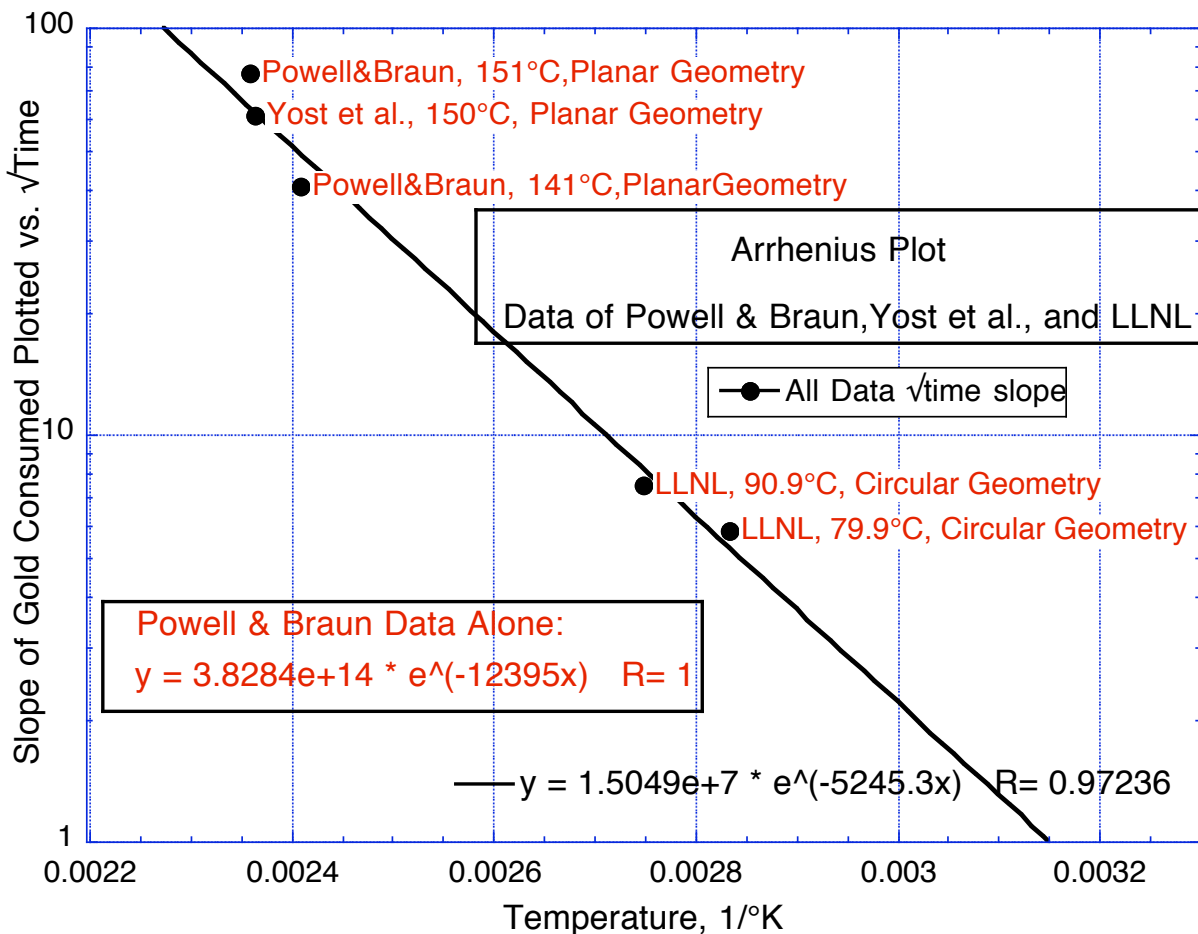


Figure 31. The coefficient multiplying " $\sqrt{\text{time}}$ " derived from figures 29 and 30 plotted vs. reciprocal temperature in degree Kelvin.

The exponential fit to the data shown in the Arrhenius plot (figure 31) determines the equation describing the rate of the diffusion-controlled reaction as a function of time. The activation energy is 5245.3 in units of degree Kelvin, in contrast to the higher activation energy for the "linear reaction", i.e. 7990, in units of °K. The activation energy determined here is derived from data over a relatively narrow temperature range, using data from planar geometry and from circular geometry. As shown in the graph: if only data of Powell & Braun were used, an activation energy of 12395 (in units of degree Kelvin) would result, with a vastly different pre-

exponential factor.

As indicated in figure 31, this model equation for the diffusion-controlled reaction is generated from only a few data points, and hence subject to revision by additional data.

C III.) Defining the temperature and time regimes where the interface and the diffusion controlled reaction models apply.

Figure 1 already suggests, that the change from interface control to diffusion control is temperature dependent. Figure 29 demonstrates - for temperatures around 150°C - at which time and gold consumption predicted by the linear reaction model intersects the observed square root of time dependent gold consumption. The linear model intersects the data at 142°C at about 22 μm , and the data at 150°C and 151°C at 34 and 55 μm respectively.

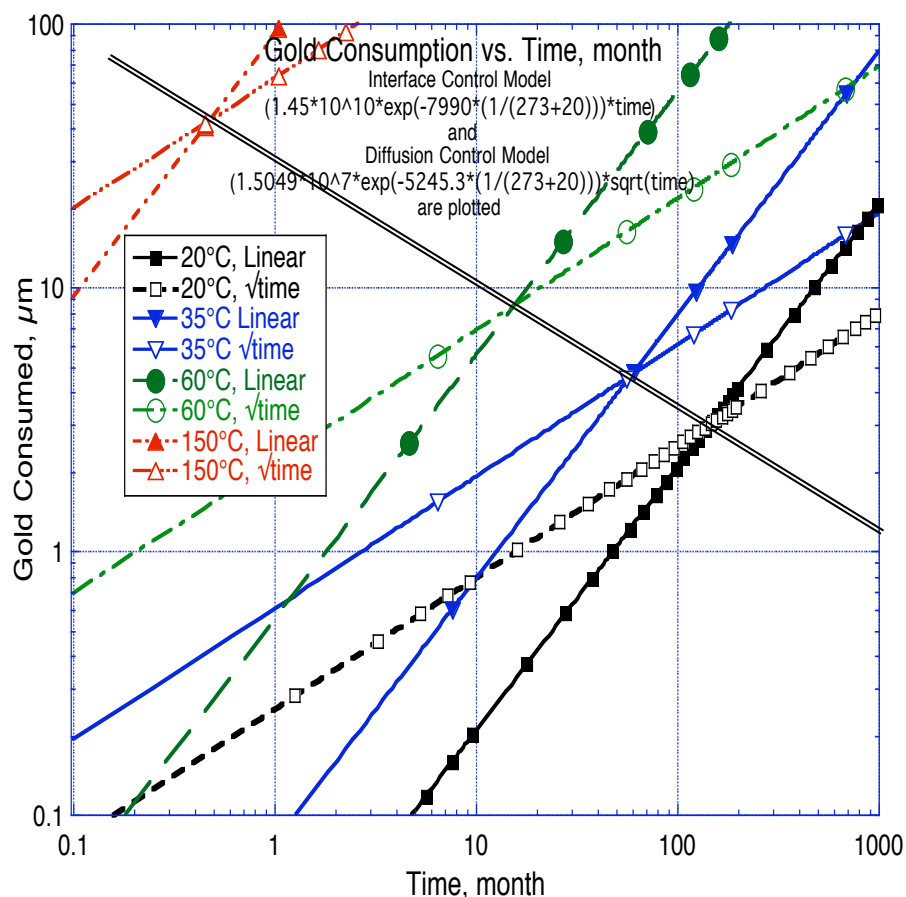


Figure 32. Gold consumption vs. time calculated using both the linear and " $\sqrt{\text{of time}}$ " model and showing the intercepts of the linear reaction model and the "square root of time dependent" model at 20, 35, 60 and 150°C.

. Figure 32 shows the intercepts of the linear reaction model and the "square root of time dependent" model at 20, 35, 60 and 150°C. The double line in the graph connects the intersect points. In the region above that line the reaction is diffusion controlled, below that line it is interface controlled. The "square root of time dependent" model derived from the data at elevated temperature predicts that at 35 and 20°C the reaction may become diffusion controlled for gold consumption less than 10µm. There are no data (see figure 1) that would contradict that prediction. Braun and Rhinehammer's data in figure 1 at 70° indicate a change in reaction mechanism occurs for gold consumption less than 10µm, just as is seen in this figure at 60°C.

The "square root of time dependent" model derived from the data at elevated temperature (see figure 31) predicts that at 35 and 20°C the reaction may become diffusion controlled for gold consumption less than 10µm. There are no data (see figure 1) that would contradict that prediction. Moreover, Braun and Rhinehammer's data in figure 1 at 70° indicate that a change in reaction mechanism may occur for gold consumption less than 10µm, just as is seen in figure 32 at 60°C. A general equation for deciding whether the reaction is interface controlled or diffusion controlled can be derived by determining the point in temperature and time when the amount of gold converted is the same in both equations, as shown below:

$$\Delta_{Gold} = A_{Linear} e^{-B_{Linear}/T} * time(month) =$$

$$\Delta_{Gold} = A_{SquareRoot} e^{-B_{SquareRoot}/T} * \sqrt{time(month)}$$

With $A_{\text{Linear}} = 1.45 * 10^{10}$, $A_{\text{Square Root}} = 1.5049 * 10^7$

$$B_{\text{Linear}} = 7990, B_{\text{Square Root}} = 5245.3$$

$$T(^{\circ}\text{K}) = 273.15 + \text{temperature } ^{\circ}\text{C}$$

and $\Delta_{\text{Gold}} = \mu\text{m of gold consumed}$

the gold - indium reaction is described by

$$\Delta_{\text{Gold}} = A_{\text{Linear}} e^{-B_{\text{Linear}}/T} * \text{time}(\text{month})$$

$$\text{for } \Delta_{\text{Gold}} \leq \left(\frac{A_{\text{Square Root}}}{A_{\text{Linear}}} \right)^2 * \left(e^{-\frac{1}{T}(B_{\text{Square Root}} - B_{\text{Linear}})} \right)^2$$

$$\Delta_{\text{Gold}} = A_{\text{Square Root}} e^{-B_{\text{Square Root}}/T} * \sqrt{\text{time}(\text{month})}$$

$$\text{for } \Delta_{\text{Gold}} \geq \left(\frac{A_{\text{Square Root}}}{A_{\text{Linear}}} \right)^2 * \left(e^{-\frac{1}{T}(B_{\text{Square Root}} - B_{\text{Linear}})} \right)^2$$

These equations define a comprehensive time and temperature dependent model for all times and temperatures.

IV.) Comparison of LLNL derived gold-indium reaction kinetics with reaction kinetics derived by Millares¹ (Millares 1993) (based on the model by Dybkov (Dybkov 1986)²).

Said model accounts for both interfacial reaction and diffusion controlled reaction *in planar geometry*, and states that at any time t , the following equation applies:

$$t = e/K_1 + e^2/K_p, \quad e = \sqrt{t^* K_p + (K_p/2K_1)^2} - (K_p/2K_1), \quad \text{Millares, equ. [1]}$$

where e is the reaction layer thickness, and K_p and K_1 are the parabolic growth rate constants for diffusion-controlled growth and linear growth rate constants for inter-facially controlled growth, respectively. This model makes the assumption that even at a reaction time when the rate of arrival of reactants to the surface is controlled and limited by the rate of diffusion through the reaction product layer of thickness " e ", the time needed to form the reaction product at the surface (here gold with the reactant indium) is still important in the rate of growth of the reaction product layer. That is debatable or questionable. Let us assume that the diffusion-controlled rate of arrival of indium atoms at the gold surface is $2/\text{cm}^2\text{s}$, and that another .5 seconds is needed to convert these indium atoms to AuIn_2 . How many AuIn_2 molecules will be formed per hour, 3600s? Will it be 3600 or $3600/1.5 = 2400$? 3600 appears more likely, because the conversion time of .5s occurs while the interface is "waiting" for the arrival of the next reactant. The Dybkov model, in contrast, would say 2400.

Millares et al. derive temperature dependent values for K_1 and K_p

¹ Millares, M. P., Bernard Lelievre, Elvire (1993).

² Dybkov, V. (1986). *The Reaction Systems for Solid State Interactions* 63-Binary-Systems .1. Growth of the Chemical-Compound Layers at the Interface between 2 Elementary Substances - One Compound Layer." *Journal of Materials Science* 21(9): 3078-3084.

from their figures 3 and 4 shown below, but do NOT indicate HOW that is done. Those values are shown in Millares' table 1 below, copied from Ref. 1.

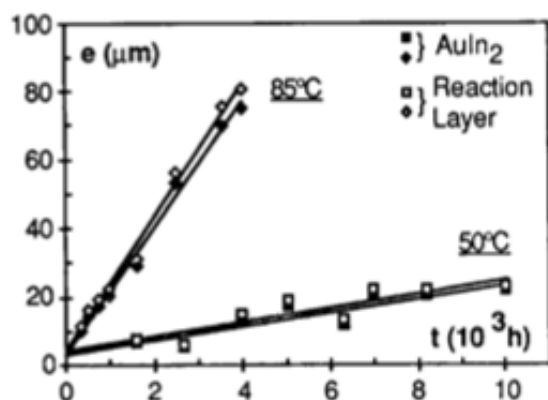


Figure 3:
Kinetics of Au-In reaction at 50 and 85°C.

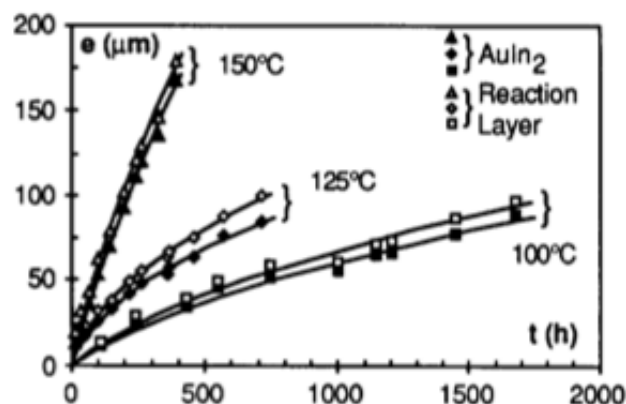


Figure 4:
Kinetics of Au-In reaction at 100, 125 and 150°C.

T (°C)	AuIn ₂ layer		Reaction layer	
	K _l (μm h ⁻¹)	K _p (μm ² h ⁻¹)	K _l (μm h ⁻¹)	K _p (μm ² h ⁻¹)
50	0,002	/	0,0021	/
85	0,019	/	0,0195	/
100	0,111	8,05	0,132	9,29
125	0,507	13	0,594	17,9
150	0,579	250	0,736	197

Table 1:
Growth rate parameters for the Au-In reaction.

As the table states, "e" is the thickness of the AuIn₂ layer. To confirm/check up on the values of K_p and K_l in Millares' table 1, the data in Millares' figure 3 and 4 were digitized, using the software "UnscanIt"³. Below the times t (hour) are plotted versus the values of AuIn₂ thickness "e" thus derived for all temperatures listed in Millares' table 1, and a function

$$t = (1/m_1) * e + (1/m_2) * e^2$$

³ Silk Scientific, Inc. | P.O. Box 533 | Orem, Utah 84059 USA

is fitted to the data. In figure 33 to 37, and in the accompanying text, "m1" and "m2" stand for Millares' K1 and Kp, respectively.

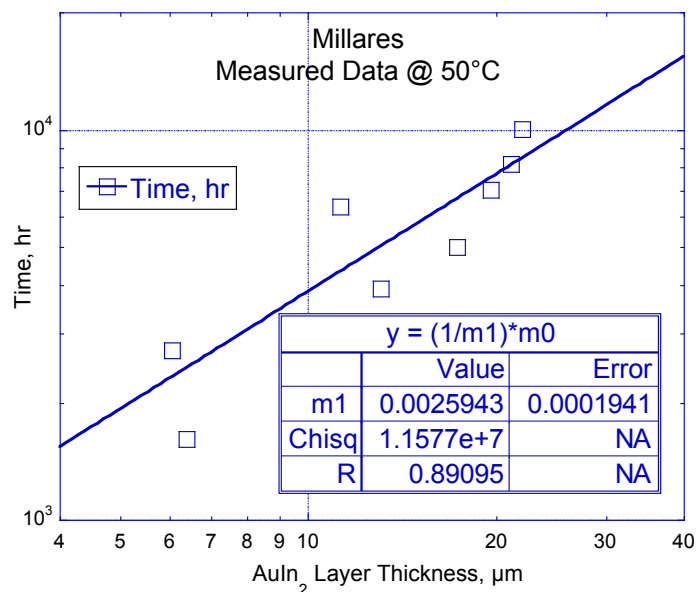


Figure 33. Time vs. gold layer thickness consumed at 50°C, using Millares's data of their figure 3. Here only m1 is used.

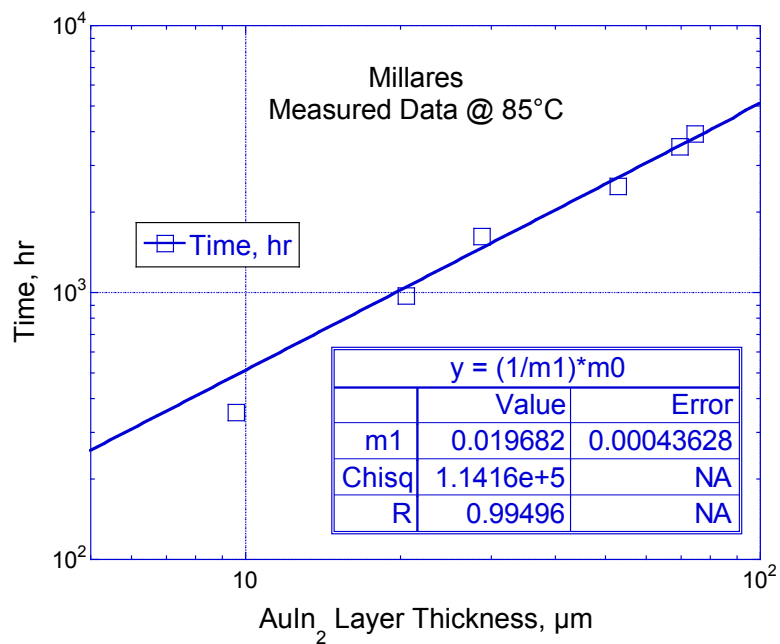


Figure 34. Time vs. gold layer thickness consumed at 85°C, using Millares's data of their figure 3. Here only m1 is used.

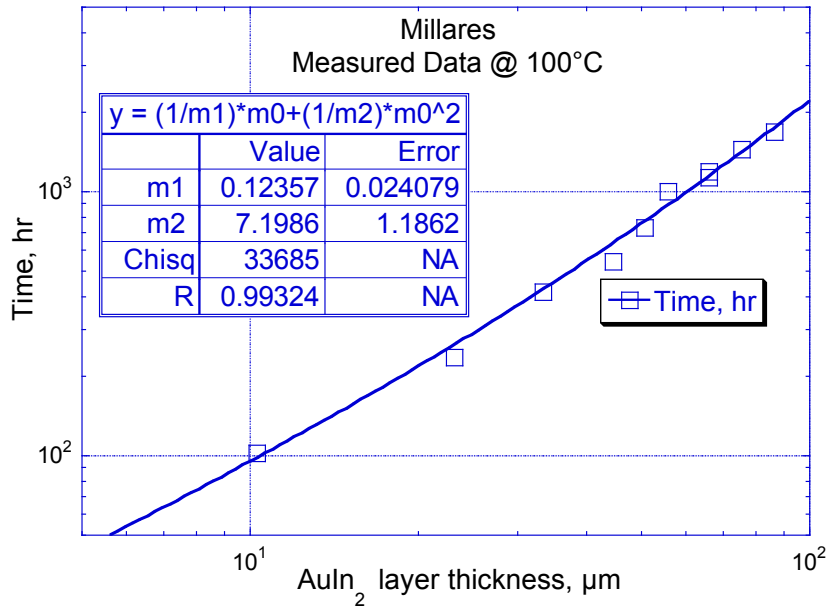


Figure 35. Time vs. gold layer thickness consumed at 100°C, using Millares's figure 4. Here both m1 and m2 are used.

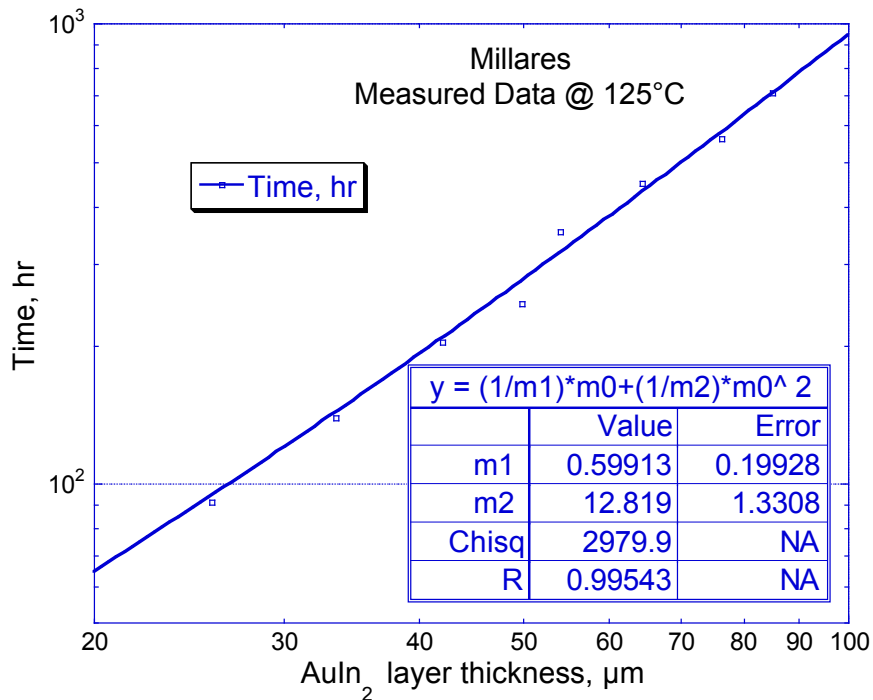


Figure 36. Time vs. gold layer thickness consumed at 125°C, using Millares's figure 4. Here both m1 and m2 are used.

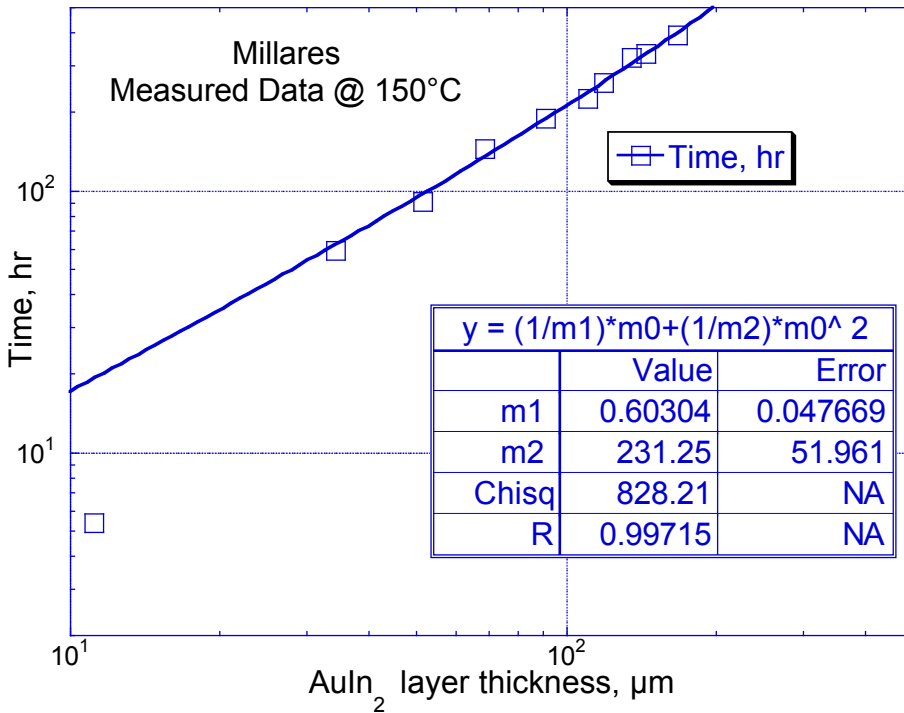


Figure 37. Time vs. gold layer thickness consumed at 150°C, using Millares's figure 4. Here both m1 and m2 are used.

Temperature, °C	AuIn2 layer			
	K1, μm h ⁻¹	K1, μm h ⁻¹	Kp, μm ² h ⁻¹	Kp, μm ² h ⁻¹
	LLNL fit	Millares	LLNL fit	Millares
50	.00259	.002	/	/
86	.0197	.019	/	/
100	.124	.111	7.2	8.05
125	.599	.507	12.82	13
150	.60304	.579	231.25	250

C IV) Table 1. Comparison of LLNL and Millares fit of K1 and Kp.

C IV) Table 1 shows that the LLNL fit to Millares' data is close to Millares' values, except for K1 at 125°C. The LLNL fit to the data at 125°C (figure 36) has an "R" value of .997, and a Kp value of 12.82, very close to Millares' 13, hence it is difficult to see how Millares' K1 value .507 (vs. LLNL's .599) was arrived at.

Figure 38 shows the activation energy of K1 and Kp derived from a plot of K1 and Kp versus inverse temperature in degree Kelvin. Both sources of data, as shown in Millares' table 1, and as derived from LLNL fits to Millares' data (his figure 3 and 4) are plotted. Exponential fits to those two data sets show little difference, as expected from C IV) table 1 above. Therefore, the fit to Millares' data will be used from now on.

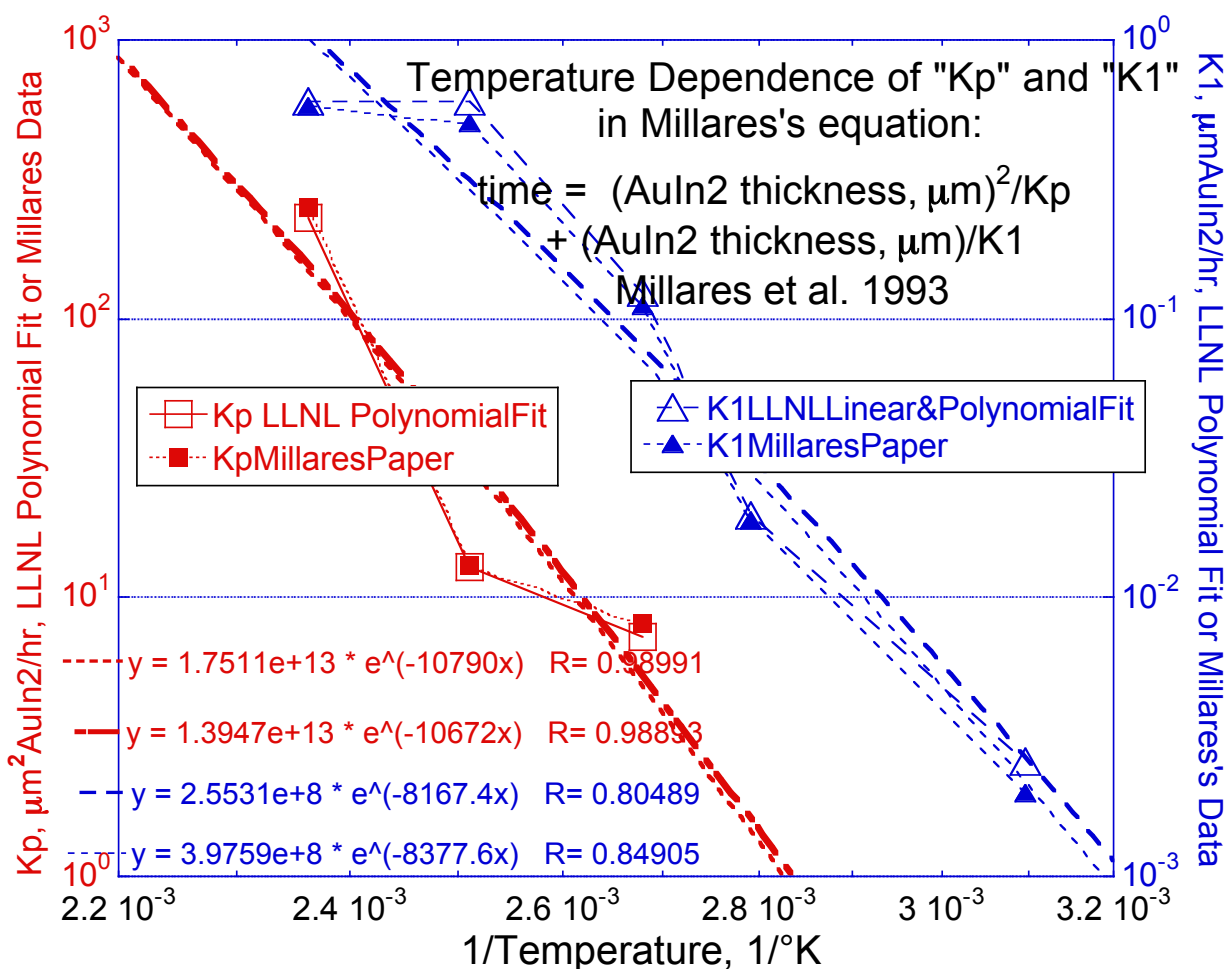


Figure 38. The activation energy of K1 and Kp derived from a plot of K1 and Kp versus inverse temperature in degree Kelvin. K1 and Kp are plotted both as shown in Millares' paper and as derived from LLNL fits to the data in Millares' figure 3 and 4. Exponential fits to both sources of data are made.

To compare Millares' reaction data with LLNL's of part A for the linear reaction and of part C.III for the non-linear reaction, one has to convert Millares' coefficients "K1" and "Kp" to the time and reaction units used in section A, i.e. time (month), and gold consumed (μm) rather than AuIn2 layer thickness. The ratio of AuIn2 layer thickness formed to gold thickness consumed is 4.2, see section A. After this conversion, the coefficients will be called "K1AuMonthMillaresData" and "KpAuMonthMillaresData".

Millares' equation is

$$t = e / K_1 + e^2 / K_p,$$

It is important to recognize that in Millares' analysis both the interface control (linear with time, K1) and the diffusion control (K2) act together at all times. In contrast, in this report the reaction is split into two parts: 1) the time period when the reaction is linear with time, and 2) the time when the reaction proceeds proportional to time. Hence, the coefficient derived in part A of this report for the "linear" reaction, and in part C.II) for the "nonlinear" reaction are not directly comparable to Millares' K1 and Kp.

In part A LLNL's linear reaction is described by

$$\Delta R(\text{gold wire radius loss, } \mu\text{m}) = 1.45 \cdot 10^{10} \cdot \exp(-7990/T\{^\circ\text{K}\}) \cdot \text{reaction time(month)}$$

or

$$\text{reaction time} = 1 / [(1.45 \cdot 10^{10} \cdot \exp(-7990/T\{^\circ\text{K}\})) \cdot (\Delta R_{\text{loss}})]$$

or, in Millares' terminology

$$\text{time} = \Delta R / [K1 \cdot \text{AuMonthLLNL}]$$

but stressing again, by use of the "*" symbol, that

K1AuMonthLLNL is NOT exactly equivalent in meaning to K1AuMonthMillaresData.

LLNL's formula in the "nonlinear regime" (see above) is

$$\Delta R = 1.5049 \cdot 10^7 \cdot \exp(-5245.3/T) \cdot \sqrt{\text{time}(\text{month})}, \text{ hence}$$

$$\text{time}(\text{month}) = \Delta R^2 / [1.5049 \cdot 10^7 \cdot \exp(-5245.3/T)]^2$$

or, in Millares' terminology

$$\text{time} = \Delta R^2 / [Kp \cdot \text{AuMonthLLNL}]$$

The resulting coefficients "K1AuMonthMillares" and "KpAuMonthMillares" of Millares, and the coefficients of the linear and nonlinear equation of this report, called "K1*AuMonthLLNL" and "Kp*AuMonthLLNL" are plotted as an Arrhenius plot in figure 39 below as a function of (1/°Kelvin).

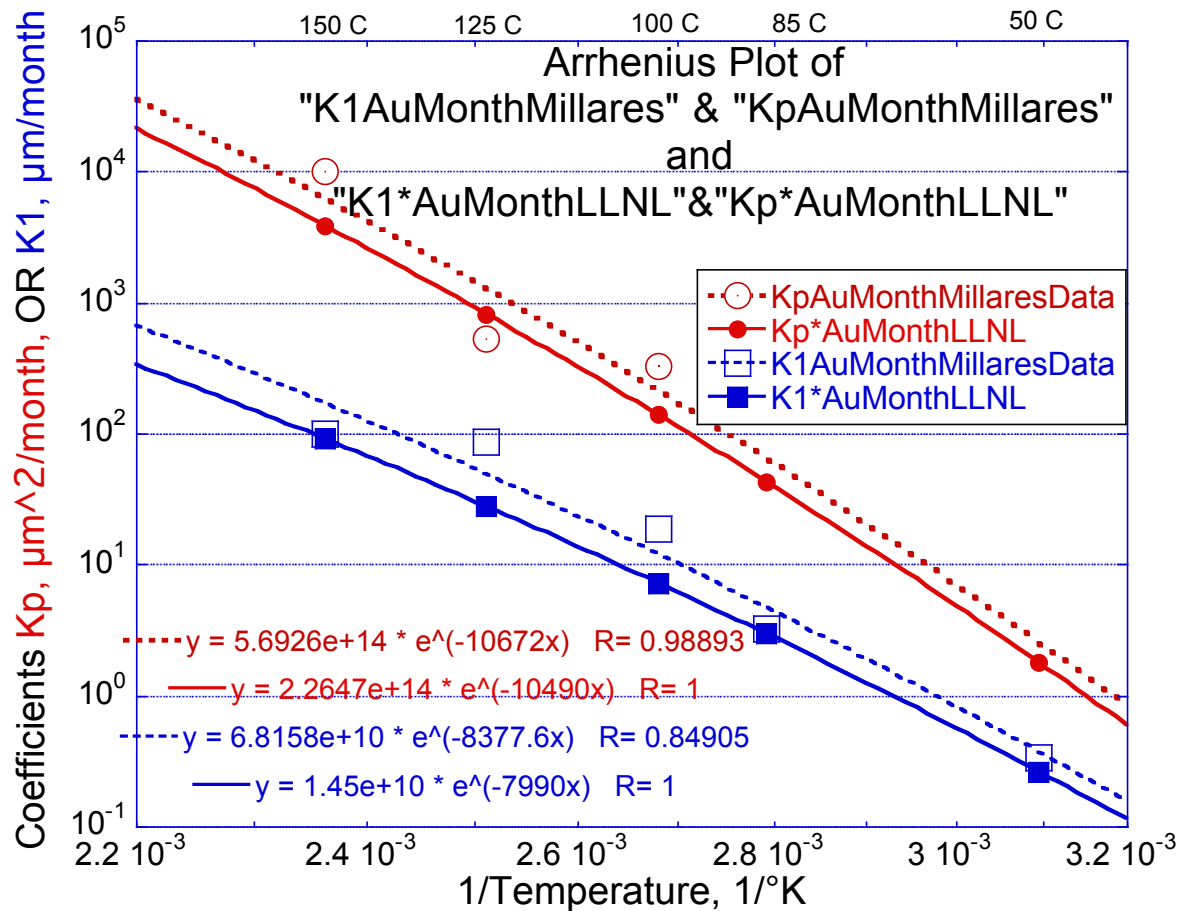


Figure 39. Arrhenius plot of K1 and Kp and K1* and Kp*, respectively, ($\mu\text{m}/\text{month}$ and $\mu\text{m}^2/\text{month}$), and the activation energy derived therefrom for LLNL and Millares' data.

Figure 39 gives these equations for Millares' K1 and Kp:

$$K_1 = 6.8158 \cdot 10^{10} \cdot \exp(-8377/T(^{\circ}\text{K}))$$

$$K_p = 5.6926 \cdot 10^{14} \cdot \exp(-10672/T(^{\circ}\text{K}))$$

While LLNL's K_1^* and K_p^* are as listed in part A and C.III:

$$K_1^* = 1.45 \cdot 10^{10} \cdot \exp(-7990/T(^{\circ}\text{K}))$$

$$K_p^* = 2.2647 \cdot 10^{14} \cdot \exp(-10490/T(^{\circ}\text{K}))$$

Both activation energies from LLNL and Millares are close to each other, 7990 for K_1^* vs. 8377 for K_1 and 10490 for K_p^* vs. 10672 for K_p , respectively. That is expected, since the activation energies of the interfacial and diffusional process have to be the same. But the pre-exponential factors differ substantially: $1.45 \cdot 10^{10}$ for K_1^* vs. 6.8 for K_1 and 2.3 for K_p^* vs. 5.7 for K_p respectively. K_1^* and K_p^* appear in the denominator, and hence must have lower values since each one alone, not together as in Millares' equation, determine the reaction. They have different meanings, as pointed out above, and can NOT be used in a Millares' equation together.

The reaction ΔR values at 20°C have been calculated using the equations listed above, for Millares using his equation with K_1 and K_p together, and for LLNL using K_1^* and K_p^* separately. The results are plotted in figure 40, together with ΔR values measured on gold wires of 1.5 mil and 4 mil diameter stored either at Mound Laboratories or at LLNL, respectively. As expected from his equation, Millares' prediction shows a continuously decreasing slope that even at 400 month (see figure 40 a) has not yet decreased to a value of .5, i.e. diffusion control; figure 40 b) extends time to 1200 month. Millares' prediction stays always below the measured values and LLNL's diffusion controlled equation, but approaches LLNL's diffusion controlled line asymptotically, as expected. LLNL's "linear reaction" equation is close to the measured values below 140 month, and the "nonlinear reaction" equation is close to the

values after ~140 month. Figure 32 showed that the transition from interface control to diffusion control occurs at approximately 140 month reaction at 20°C.

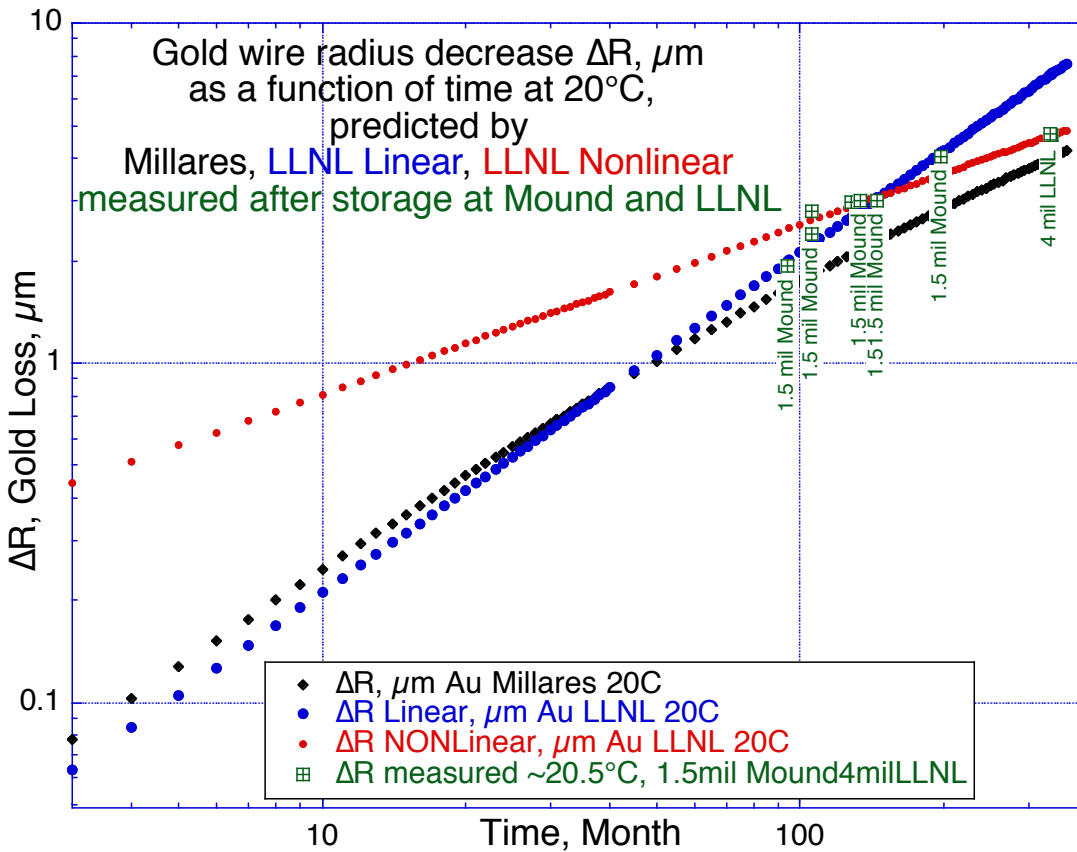


Figure 40 a. Gold wire radius decrease Δr , μm , as a function of time (up to 400 month) at a reaction temperature of 20°C as predicted by Millares or LLNL, and as measured after storage at Mound or LLNL at $\sim 20^\circ\text{C}$.

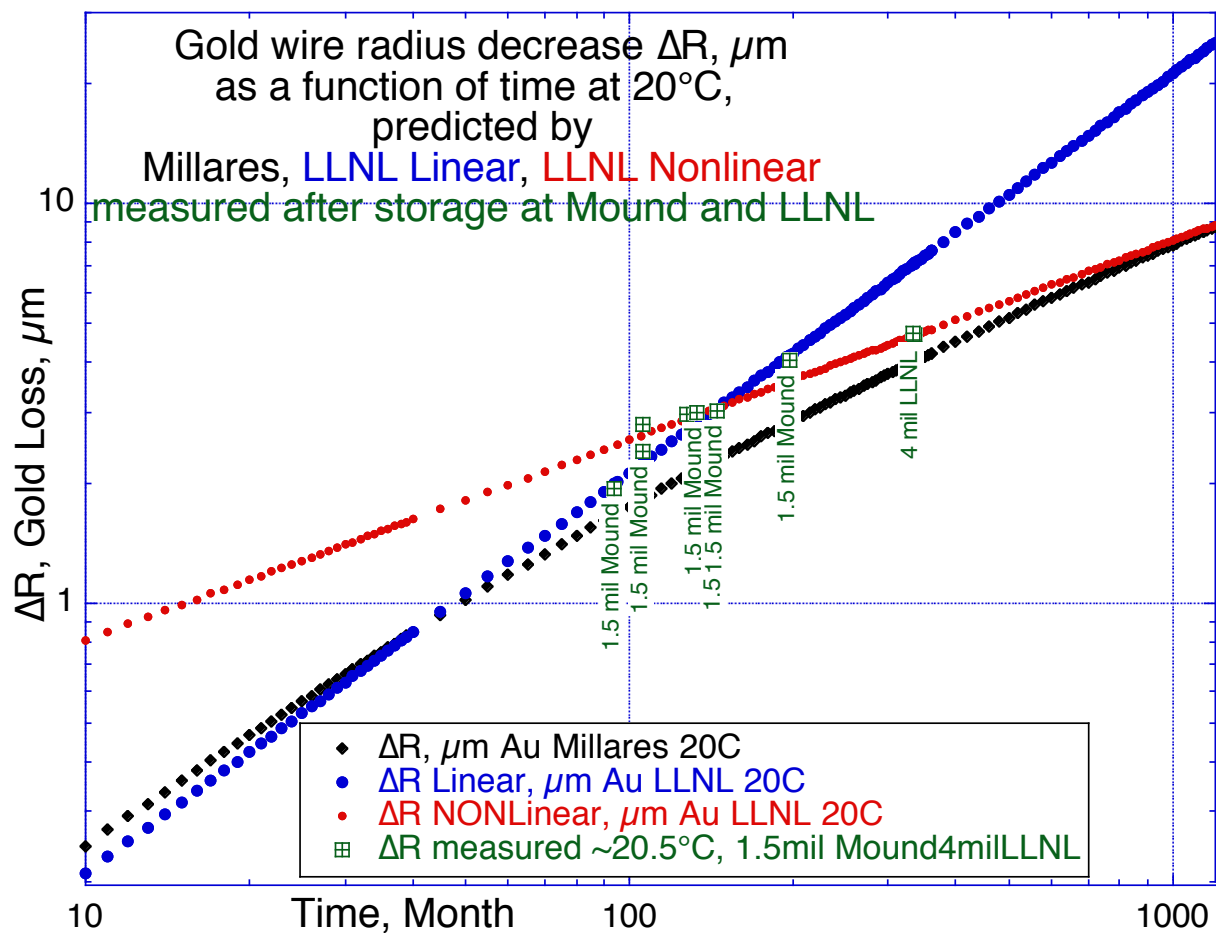


Figure 40 b. Gold wire radius decrease Δr , μm , as a function of time (up to 1200 month) at a reaction temperature of 20°C as predicted by Millares or LLNL, and as measured after storage at Mound or LLNL at $\sim 20^\circ\text{C}$. Millares' equation approach LLNL's Nonlinear (diffusion control) equation asymptotically, as expected.

C V.) Summary

We have developed a model for the diffusion controlled reaction, and defined the regime where it applies. It is based on very few data, and hence possibly subject to revision as new data are generated. It predicts a slower rate of gold conversion than the "conservative" interface controlled model. We have shown that the linear model of part A and the nonlinear model of part C, section III, agree with measurements of gold wire radius decrease ΔR held at 20°C for up to 340 month.

Having defined the regimes where the interface controlled model applies, and where the diffusion controlled model supersedes it, we derived the set of equations of a comprehensive reaction model that applies for all temperatures and times and agrees with ΔR measurements at 20°C over extended time. We compare this model with the model published by Millares et al. and find that our reaction equations provide in cylindrical geometry a better fit in the diffusion controlled regime.